MATHEMATICAL BIOSCIENCES
AND ENGINEERING
Volume **12**, Number **1**, February **2015**

doi:10.3934/mbe.2015.12.135

pp. **135–161**

ANALYSIS OF SI MODELS WITH MULTIPLE INTERACTING POPULATIONS USING SUBPOPULATIONS

Evelyn K. Thomas

Department of Mathematics and Statistics
University of Maryland Baltimore County
Baltimore, MD 21250, USA

Katharine F. Gurski

Department of Mathematics, Howard University
Washington, DC 20059, USA

Kathleen A. Hoffman

Department of Mathematics and Statistics
University of Maryland Baltimore County
Baltimore, MD 21250, USA

(Communicated by Zhilan Feng)

Abstract. Computing endemic equilibria and basic reproductive numbers for systems of differential equations describing epidemiological systems with multiple connections between subpopulations is often algebraically intractable. We present an alternative method which deconstructs the larger system into smaller subsystems and captures the interactions between the smaller systems as external forces using an approximate model. We bound the basic reproductive numbers of the full system in terms of the basic reproductive numbers of the smaller systems and use the alternate model to provide approximations for the endemic equilibrium. In addition to creating algebraically tractable reproductive numbers and endemic equilibria, we can demonstrate the influence of the interactions between subpopulations on the basic reproductive number of the full system. The focus of this paper is to provide analytical tools to help guide public health decisions with limited intervention resources.

1. **Introduction.** There have been several examples in which the quantitative fields of mathematics and statistics have significantly impacted the life sciences; namely, the area of ecology and population biology. From the simple exponential growth of a population of bacteria to the seminal equations of Lotka [29, 30, 31] and Volterra [59, 60], the use of mathematical models to understand population dynamics has significantly impacted the way biologists view these areas. The Lotka-Volterra predation equations successfully captured the oscillations and phase shift between the predator population and the prey population of the Hudson Bay Company pelt trading data that spans almost a century [15, 45]. Since Lotka and Volterra's time, scientists have expanded on their fundamental contributions including spatial-temporal effects, age-structured populations, and even studied the

2010 *Mathematics Subject Classification.* Primary: 92D30; Secondary: 37C75.

Key words and phrases. Reproductive number, stability, SI model, compartmental model, spread of HIV.

effect of harvesting on fish populations [3, 35, 51, 54] and the impact of forest fires on flora and fauna [32]. One particularly important field within population dynamics is that of epidemiology, in which the the populations are structured according to their disease status, particularly the susceptible, infected, and recovered categories (see for example, [1, 5, 19, 24, 25, 26]). These types of population models have been used to study the spread of the Black Death that swept through Europe in the mid 1300s [36, 41], gonorrhea [13, 18, 27], HIV [6, 8] (among many other references), and cholera [10, 11, 16]. With the development of biochemical weapons and the onset of potential global epidemics of swine flu (H1N1) and SARS, understanding epidemiological models is becoming more important from a national security and public health perspective.

This paper focuses on a new method for constructing analytical tools that will help target intervention and vaccination strategies by analyzing the basic reproductive numbers of the subpopulations of a system to reduce the size (or delay the onset) of the endemic equilibria of chronic diseases. The practical implication behind the study of epidemiological models is to identify which strategies best control the spread of disease. In practice there are limited resources that can be allocated for education, prevention, and treatment which means it is imperative to determine the most effective methods of intervention and vaccination strategies to eradicate and mitigate the impact of a global epidemic. Given the complexity of analytical results of systems with multiple couplings, recommendations are traditionally based on numerical simulations in which the biological parameters are varied. A more practical solution provides analytical bounds on the basic reproductive number and approximations to the endemic equilibrium. Our analytical bounds can be used to easily identify which subpopulation to target to achieve the best result with limited resources. Our goal is to develop mathematical tools to aid medical practitioners and assist organizations in planning points of intervention.

Our analysis was motivated by modeling incurable sexually transmitted diseases using a simple SI model (S represents the susceptible population and I represents the infected category) for three subpopulations. The full model consisted of six nonlinear differential equations with seventeen different parameters (see Figures 1 and 2, Table 1, and Eq (1) for specifics of the models and parameters). Computing the endemic equilibrium and basic reproductive numbers of this system is algebraically intractable, specifically if one is designing intervention strategies targeted at reducing the size of the endemic equilibrium or the basic reproductive number.

Our motivational model consists of a susceptible and an infected population for each of three subpopulations: heterosexual females, heterosexual males, and bisexual males. Previously, a series of papers written by Mukandavire et al, [33, 39, 40], considered a model, similar to the one we consider with fewer connections between subpopulations, and focused on the basic reproductive number of the disease. In contrast, we developed a method for bounding the basic reproductive number of the disease in terms of the basic reproductive number of groups of subpopulations within the system. The motivation for the sexual couplings depicted in this model stem from a modification of the interactions presented in the Mukandavire study, consisting of bisexual males, heterosexual females, and heterosexual males. We consider the basic reproductive number of the bisexual males as an isolated system and the basic reproductive number of the heterosexual males and heterosexual females as an isolated system, then use these numbers to bound the basic reproductive number of the full system including all three populations. The basic reproductive numbers

of the disease within these subpopulations are useful in quantifying a metaphorical *bridge* between decoupled subsystems.

We also propose a method in which the values of the endemic equilibria of the subsystems are used as nonhomogeneous forcing terms to the remaining populations. This alternate formulation provides an analytically tractable system, with explicit expressions for the endemic equilibrium, that approximates the dynamics of the full system. In particular, we provide numerical simulations showing the relationship of the alternate system to the dynamics of the full system and an analytic bound on the basic reproductive number of the full system in terms of the basic *reproductive-like* number (to be defined in section 6) of the subsystems.

In section 2 we present the full S-I model for three populations. In section 3 we deconstruct the system into smaller subsystems and examine the dynamics of these subpopulations. In section 4 we show how the analytical results from the subsystems describe and bound the basic reproductive number of the full system. In section 5 we present the endemic equilibrium of the full system in terms of the basic reproductive numbers of the subsystems. In section 6 we introduce a third system which approximates the interactions between populations with terms that reflect the influence from the other subsystems and discuss disease stability in terms of *reproductive-like* numbers of the subsystems. We include a comparison of the endemic equilibrium from the directly connected system and the system with influence terms. In section 7 we apply the model and methods to describe the HIV infection. Lastly in section 8 we present the conclusions and a discussion of our analysis.

2. **Full model.** In this section, we develop an SI model of three generic populations A, B, C, whose interactions are motivated by the three interacting subpopulations: bisexual males, heterosexual females, and heterosexual males, described in the introduction, for a model of an incurable sexually transmitted disease, such as HIV. We introduce a standard SI model with three subpopulations to set notation. We further describe two subsystems: one consisting of population A, corresponding to the bisexual population, and a second system consisting of populations B and C, corresponding to the heterosexual females and males, respectively. We describe the dynamics of each subpopulation including the reproductive number for each which forms the foundation for bounding the reproductive number of the full system, addressed in section 4.

In Figure [1], the three populations enter the susceptible population at a rate of $p_j\Lambda$, where $j = A$, B, or C; this can be seen in the arrows pointing into the susceptible compartments of each population. Once the disease is passed, individuals move from the susceptible populations to the infective population by their respective forces of infections, θ_j. Individuals can leave the infected population with removal rate $\delta_j = \mu_j + d_j$, where μ_j represents disease induced removal rate and d_j represents the natural death rate. The definition of the disease removal rate depends upon its context within the disease: it could represent disease-death or progression to another stage of the disease. Table 1 summarizes the notations and constants.

The model corresponding to the SI structure illustrated in Figure [1] is given below:

$$\frac{dS_j}{dt} = p_j\Lambda - \theta_j S_j - d_j S_j, \tag{1}$$

TABLE 1. Notation for the variables that describe each population.

Symbol	Description
S_j	Susceptible individuals in population j
I_j	Infected individuals in population j
N_j	Total population of j
N	Total population
b_{ij}	Probability of infection per exposure in population i to an individual in population j
c_{ij}	Contact number of an individual in population i with a new individual in population j.
$\psi_{ij} = c_{ij}b_{ij}$	Transmission rate from an individual in population i to an individual in population j
p_j	Proportion of population j entering into susceptible population
Λ	Recruitment rate into susceptible population
μ_j	Death rate due to disease of individuals in population j
d_j	Natural death rate of individuals in population j
$\delta_j = \mu_j + d_j$	Total death rate of individuals in population j

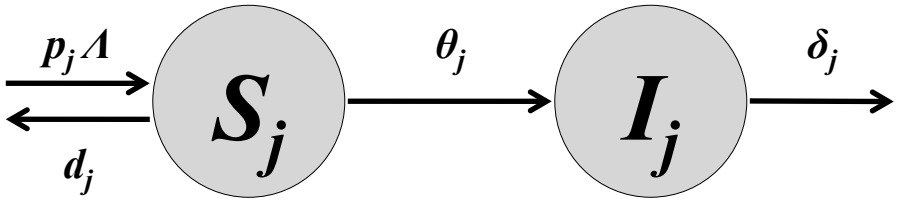

FIGURE 1. Basic S-I Model.

$$\begin{aligned} \frac{dI_j}{dt} &= \theta_j S_j - \delta_j I_j, \\ \frac{dN_j}{dt} &= p_j\Lambda - d_j S_j - \delta_j I_j. \end{aligned}$$

We consider a system with three populations, i.e. $j = A, B, C$. Each population A, B, C has the susceptible-infected (SI) structure illustrated in Figure 1. The interaction terms are not immediately obvious, these are part of the force of infection θ_j where $j = A, B, C$. These θ_j terms capture the interactions between the populations as illustrated in Figure 2. The choice of this particular interaction was motivated by modeling the incurable sexually transmitted diseases with bisexual males (population A), heterosexual females (population B), and heterosexual males (population C). In this figure, we see that population A, bisexual males in the example, interact with themselves, as well as with population B, heterosexual females, and the heterosexual males and heterosexual females interact with each other. This choice of interactions between subpopulations gives explicit forms of the forces of infections:

$$\theta_A = \frac{\psi_{AA} I_A}{N_{AC}} + \frac{\psi_{BA} I_B}{N_B}, \quad \theta_B = \frac{\psi_{CB} I_C}{N_{AC}} + \frac{\psi_{AB} I_A}{N_{AC}}, \quad \theta_C = \frac{\psi_{BC} I_B}{N_B}, \tag{2}$$

where $N_{AC} = N_A + N_C$. The dashed rectangles in Figure 2 delineate how the three population system is deconstructed into System I and System II.

Hence

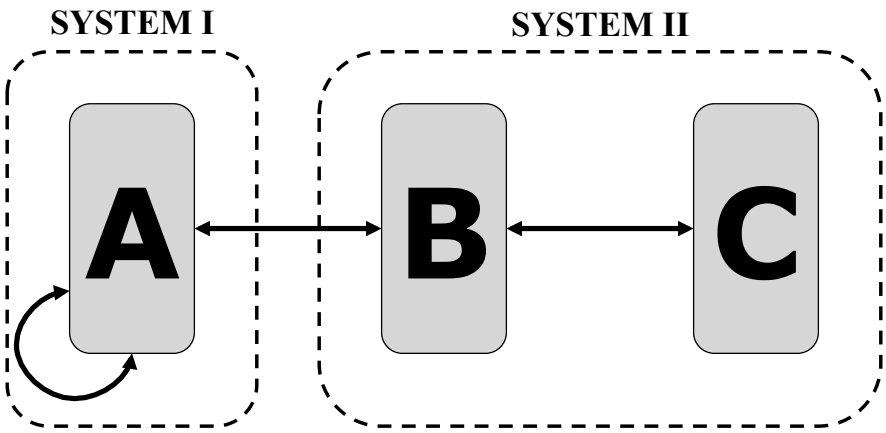

FIGURE 2. Three Population Model: Interactions between populations A, B, and C.

For chronic diseases, $\mu_j \approx 0 \ \forall j \in \{A, B, C\}$, then $d_j \approx \delta_j$. Consequently, our expression for the rate of change of size of the subpopulations with respect to time can now be rewritten as: $\frac{dN_j}{dt} = p_j \Lambda - \delta_j N_j$. It follows as $t \to \infty$, $N_j(t) \to \frac{p_j \Lambda}{d_j} = N_j^*$. The theory of asymptotically autonomous systems, in particular a result of Thieme [56, p. 385-387], allows us to reduce the large-time behavior of system (1) to a simpler set of equations exploiting the constant subpopulations. Namely, let $x = 1 - s_A$, $y = 1 - s_B$, and $z = 1 - s_C$ where $s_j = S_j/N_j$, $x = I_A/N_A$, $y = I_B/N_B$, and $z = I_C/N_C$. Correspondingly we rescale the transmission rates as $\beta_{Aj} = \psi_{Aj} N_A/N_{AC}$, $\beta_{Bj} = \psi_{Bj}$, and $\beta_{CB} = \psi_{CB} N_C/N_{AC}$. To capture the relationships of the full system we need only consider the smaller system of infected classes:

$$\frac{dx}{dt} = (\beta_{AA} x + \beta_{BA} y)(1 - x) - \delta_A x, \tag{3}$$

$$\frac{dy}{dt} = (\beta_{CB} z + \beta_{AB} x)(1 - y) - \delta_B y, \tag{4}$$

$$\frac{dz}{dt} = \beta_{BC} y (1 - z) - \delta_C z. \tag{5}$$

The susceptible populations can be reconstructed using the relations $s_A = 1 - x$, $s_B = 1 - y$, and $s_C = 1 - z$.

3. **Dynamics of subpopulations.** Even with the reduced form of the equations of the full system given by Eqs. (3-5), the number of parameters in the system makes the calculation and computation of the endemic equilibrium and the basic

reproductive number algebraically intractable. In this section we introduce two subsystems as depicted in Figure 2. For each of these subsystems we will compute both endemic equilibria and basic reproductive numbers. The basic reproductive numbers of these smaller systems will be used to bound the basic reproductive number of the full system and the values of the endemic equilibria will be used to compute a nonhomogeneous forcing term in the alternate formulation discussed in section 6.

We will reserve the term $\mathcal{R}_0$ for the basic reproductive number of the three population fully connected system and (x^*, y^*, z^*) for its endemic equilibrium. The endemic equilibria of Systems I and II will be designated as x_1^* and (y_2^*, z_2^*) respectively. The basic reproductive number for System I is $\mathcal{R}_A$, as the system consists of population A solely and the basic reproductive number for System II is $\mathcal{R}_{BC}$, as the system consists of populations B and C. The interaction number of a subsystem, τ_{AB} will later be introduced for the interactions of populations A and B.

Dynamics of System I for Population A. The dynamics of System I are governed by a single equation, Eq (3). From the Next Generation Method [7] we find the basic reproductive number

$$\mathcal{R}_A = \frac{\beta_{AA}}{\delta_A}. \tag{6}$$

The Next Generation Method ensures the local asymptotic stability of the disease-free equilibrium when $\mathcal{R}_A < 1$ and instability of this point when $\mathcal{R}_A > 1$ [7], thus the disease-free equilibrium is locally asymptotically stable when $\mathcal{R}_A < 1$. The endemic equilibrium

$$x_1^* = \frac{\mathcal{R}_A - 1}{\mathcal{R}_A}, \tag{7}$$

exists and can be shown to be locally asymptotically stable when $\mathcal{R}_A > 1$.

Dynamics of System II for Populations B and C. The dynamics of System II are governed by Eqs (4) and (5). From the Next Generation method we find the basic reproductive number,

$$\mathcal{R}_{BC} = \sqrt{\frac{\beta_{BC}\beta_{CB}}{\delta_B\delta_C}}. \tag{8}$$

Then the disease-free equilibrium is locally asymptotically stable when $\mathcal{R}_{BC} < 1$. The endemic equilibrium,

$$(y_2^*, z_2^*) = \left(\frac{\mathcal{R}_{BC}^2 - 1}{\mathcal{R}_{BC}^2 - \frac{\beta_{BC}}{\delta_C}}, \frac{\mathcal{R}_{BC}^2 - 1}{\mathcal{R}_{BC}^2 - \frac{\beta_{CB}}{\delta_B}} \right), \tag{9}$$

is globally asymptotically stable for $\mathcal{R}_{BC} > 1$ using results from [28] by showing that there exists a compact absorbing set K with a direction field pointing toward its interior and eliminating periodic orbits within the domain of our problem.

Interaction of Population A with B. Here we consider the direct interaction between population A and population B. That is,

$$\frac{dx}{dt} = \beta_{BA} y\,(1 - x) - \delta_A x, \tag{10}$$

$$\frac{dy}{dt} = \beta_{AB} x\,(1 - y) - \delta_B y. \tag{11}$$

The interaction number of population A and population B, ignoring self-interactions of population A, is

$$\tau_{AB} = \sqrt{\frac{\beta_{AB}\beta_{BA}}{\delta_A\delta_B}}. \tag{12}$$

The notation, τ_{AB} has been chosen to indicate that this is an interaction between population A and population B and not of the the full A-B system. We will use this number in bounding the basic reproductive number of the full system in the next section. The endemic equilibrium of this system is equivalent to that in Eq. (9) with the label C replaced with A.

4. **Bound on the basic reproductive number for full system.** In this section we will utilize basic reproductive and interaction numbers, $\mathcal{R}_A$, $\mathcal{R}_{BC}$, and τ_{AB}, together with other information gathered from the decoupled subsystems to obtain a bound on $\mathcal{R}_0$, the basic reproductive number of the full system.

Using the Next Generation Method the basic reproductive number is defined as $\mathcal{R}_0 = \max\{w : P(w) = 0\}$ where

$$P(w) = w^3 - \mathcal{R}_A w^2 - \left(\mathcal{R}_{BC}^2 + \tau_{AB}^2\right) w + \mathcal{R}_{BC}^2\mathcal{R}_A \tag{13}$$

and the expressions $\mathcal{R}_A$, $\mathcal{R}_{BC}$, and τ_{AB} are the basic reproductive numbers and interaction number of the deconstructed models, found in Systems I and II in Eqs (6, 8, 12). The analytical solutions of this polynomial exist, however it is difficult to get a true understanding of the factors affecting the basic reproductive number due to the length of its expression. In order to get a sense of the size of this value, we bound $\mathcal{R}_0$ in terms of reproductive numbers that are algebraically computable in the following theorem.

Theorem 4.1. *The basic reproductive number $\mathcal{R}_0$ is bounded above and below by functions of the basic reproductive numbers $\mathcal{R}_A$ and $\mathcal{R}_{BC}$ and the interaction number τ_{AB} with the following inequality:*

$$\max\left(\mathcal{R}_A, \sqrt{\tau_{AB}^2 + \mathcal{R}_{BC}^2}\right) < \mathcal{R}_0 < \mathcal{R}_A + \frac{\left(\tau_{AB}^2 + \mathcal{R}_{BC}^2\right)^2}{4\mathcal{R}_A\mathcal{R}_{BC}^2}. \tag{14}$$

Proof. Our strategy for bounding the roots of $P(w)$ is to construct two other polynomials $P_1(w)$ and $P_2(w)$, each having three real roots that can be found analytically, and bound $P(w)$ above and below, respectively. Figure 3 illustrates all three polynomial functions $P_1(w) > P(w) \geq P_2(w)$. On figure 3 the basic reproductive number $\mathcal{R}_0$ is bounded above by a root of $P_2(w)$ given by $\left(\mathcal{R}_A + \frac{(\tau_{AB}^2+\mathcal{R}_{BC}^2)^2}{4\mathcal{R}_A\mathcal{R}_{BC}^2}\right)$ and below by a root of $P_1(w)$ labeled T in the figure.

We begin by defining the polynomial $P_1(w)$, representing a lower bound on the roots of $P(w)$. Define the function

$$P_1(w) = P(w) + \tau_{AB}^2\mathcal{R}_A = \left(w^2 - \left(\tau_{AB}^2 + \mathcal{R}_{BC}^2\right)\right)(w - \mathcal{R}_A) \tag{15}$$

where $P_1(w)$ is a vertical shift up from $P(w)$ by $\tau_{AB}^2\mathcal{R}_A$ units and consequently, the maximal root of $P(w)$ is greater than the maximal root of $P_1(w)$. The roots of $P_1(w)$ are $\mathcal{R}_A$ and $\pm\sqrt{\tau_{AB}^2 + \mathcal{R}_{BC}^2}$. The points S and T in the figure will correspond to the values $\mathcal{R}_A$ and the $\sqrt{\tau_{AB}^2 + \mathcal{R}_{BC}^2}$, with T being the larger of those two roots. Hence we have two cases for a maximal lower bound: $\mathcal{R}_0 > \mathcal{R}_A$ or $\mathcal{R}_0 > \sqrt{\tau_{AB}^2 + \mathcal{R}_{BC}^2}$ depending on the value of T, as illustrated in Figure 3.

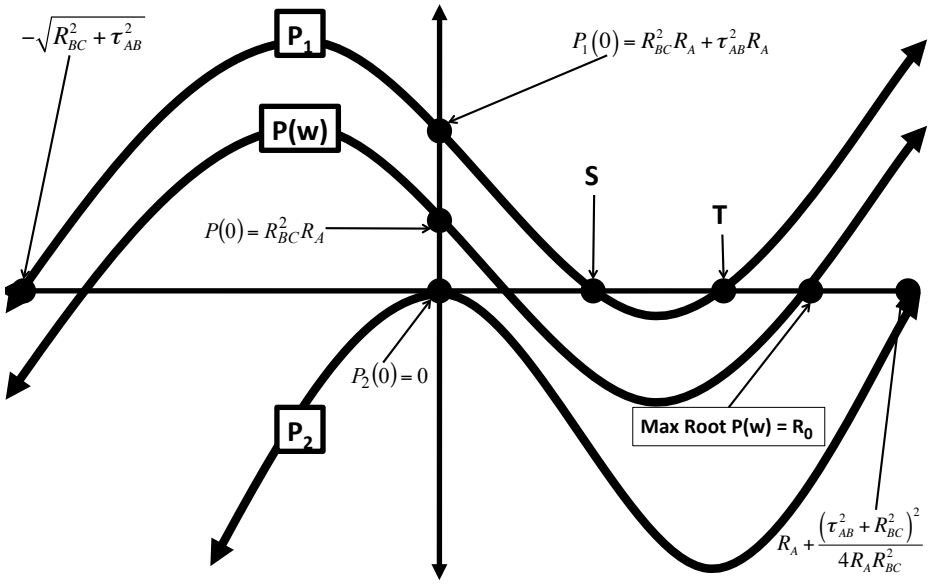

FIGURE 3. This figure displays the polynomials P_1 and P_2, whose roots are used to bound the maximal root of the function $P(w)$. The basic reproductive number $\mathcal{R}_0$ is bounded below by T whose value is the maximum of $\mathcal{R}_A$ and $\sqrt{\tau_{AB}^2+\mathcal{R}_{BC}^2}$.

Similarly we define $P_2(w)$

$$P_2(w) = w^2\left[w - \left(\mathcal{R}_A + \frac{(\tau_{AB}^2+\mathcal{R}_{BC}^2)^2}{4\mathcal{R}_A\mathcal{R}_{BC}^2}\right)\right], \tag{16}$$

whose maximum root is given by $\left(\mathcal{R}_A + \frac{(\tau_{AB}^2+\mathcal{R}_{BC}^2)^2}{4\mathcal{R}_A\mathcal{R}_{BC}^2}\right)$ and is an upper bound for $\mathcal{R}_0$. We further show

$$\begin{aligned} P(w) - P_2(w) &= \frac{(\tau_{AB}^2+\mathcal{R}_{BC}^2)^2}{4\mathcal{R}_A\mathcal{R}_{BC}^2}w^2 - \left(\tau_{AB}^2+\mathcal{R}_{BC}^2\right)w + \mathcal{R}_{BC}^2\mathcal{R}_A, \quad (17)\\ &= \frac{(\tau_{AB}^2+\mathcal{R}_{BC}^2)^2}{4\mathcal{R}_A\mathcal{R}_{BC}^2}\left(w - \frac{2\mathcal{R}_A\mathcal{R}_{BC}^2}{\tau_{AB}^2+\mathcal{R}_{BC}^2}\right)^2, \quad (18)\end{aligned}$$

which implies the curve $P(w)$ is always above or equal to the curve $P_2(w)$ and the maximum root of $P_2(w)$ is greater than or equal to the maximum root of $P(w)$. We note that for $w = \frac{2\mathcal{R}_A\mathcal{R}_{BC}^2}{\tau_{AB}^2+\mathcal{R}_{BC}^2}$, $P(w)$ equals $P_2(w)$, which is not illustrated in the figure. □

The previous theorem bounds the basic reproductive number of the disease in terms of the size of the basic reproductive numbers within the decoupled subpopulations. For example, if τ_{AB} is reduced, then the upper bound on $\mathcal{R}_0$ is reduced. This would correspond to reducing the transmission of disease between the bisexual men and heterosexual women. Thus, this analytic bound on $\mathcal{R}_0$ can be used to identify the best intervention points, with limited resources, to reduce the spread chronic diseases in the population. In terms of epidemiology, the lower bound on $\mathcal{R}_0$ represents the dependence on both secondary infections within system I and the

secondary infections within system II including an influx of disease from system I. We explore this relationship in our alternate formulation for the full system shown in section 6. The maximal bound for $\mathcal{R}_0$ represents the secondary infections within system I along with a ratio of secondary infections in system II caused by members of system II to the secondary infections in system II caused by members of system I. This is seen by the inequalities

$$\mathcal{R}_A + \frac{(\tau_{AB}^2 + \mathcal{R}_{BC}^2)^2}{4\mathcal{R}_A\mathcal{R}_{BC}^2} \leq \mathcal{R}_A + \frac{(\tau_{AB}^2 + \mathcal{R}_{BC}^2)^2}{4\tau_{AB}^2\mathcal{R}_{BC}^2} = \mathcal{R}_A + \frac{\tau_{AB}^4}{\tau_{AB}^2\mathcal{R}_{BC}^2} < \mathcal{R}_A + \frac{\tau_{AB}^2}{\mathcal{R}_{BC}^2},$$

whenever $\mathcal{R}_{BC}^2 < \tau_{AB}^2 < \mathcal{R}_A$. If this relationship were fully reversed, then

$$\mathcal{R}_A + \frac{(\tau_{AB}^2 + \mathcal{R}_{BC}^2)^2}{4\mathcal{R}_A\mathcal{R}_{BC}^2} \leq \mathcal{R}_A + \frac{\mathcal{R}_{BC}^4}{\tau_{AB}^2\mathcal{R}_{BC}^2} = \mathcal{R}_A + \frac{\mathcal{R}_{BC}^2}{\tau_{AB}^2}.$$

Additionally, it follows from our stability analysis these subsystems' basic reproductive numbers have an influence on the stability of the system's equilibrium, as shown in the next proposition.

Proposition 1. *We have the following necessary condition for a locally asymptotically stable disease-free equilibrium in the three population model in Eqs. (3 - 5) consisting of the A, B, and C populations when*

$$\tau_{AB}^2 < (1 - \mathcal{R}_A)(1 - \mathcal{R}_{BC}^2), \tag{19}$$

where $\mathcal{R}_A$, τ_{AB}, and $\mathcal{R}_{BC}$ are all less than 1.

In order to have a stable disease free equilibrium, we need to have $\mathcal{R}_0 < 1$. Hence, the lower bound for $\mathcal{R}_0$ given in Eq. (14) must be less than 1. Thus, $\mathcal{R}_A$, τ_{AB}, and $\mathcal{R}_{BC}$ must be all less than 1.

This expression was obtained by examining the conditions under which the Jacobian of our system evaluated at the disease-free equilibrium is negative. Note the condition $\tau_{AB}^2 < (1 - \mathcal{R}_A)\left(1 - \mathcal{R}_{BC}^2\right)$ is the same as $s(A) \leq 0$ shown in Lajmanovich and Yorke [27, Theorem 3.1, page 227] using the theory of irreducible matrices. Similarly the condition for stability of the endemic equilibrium, $\tau_{AB}^2 > (\mathcal{R}_A - 1)\left(\mathcal{R}_{BC}^2 - 1\right)$, is also a consequence of Lajmanovich and Yorke [27, Theorem 3.1, page 227] with $s(A) > 0$. Alternatively, Wang and Dai [61] use the theory of complex networks to show a similar result. Given the complexity of the basic reproductive number of the system, (19) provides an epidemiologically interpretable expression that relates the basic reproductive numbers of these subsystems. We can clearly see as τ_{AB} increases, so does the severity of the disease in either one or both of the decoupled subsystems I and II.

The basic reproductive number of the disease corresponds to the maximal root of the polynomial (13) and is dependent upon the size of the basic reproductive numbers of the subsystems, $\mathcal{R}_A$ and $\mathcal{R}_{BC}$. We numerically explore how the reproductive number of the full system changes as $\mathcal{R}_A$ and $\mathcal{R}_{BC}$ change in Figure 4. The reproductive number $\mathcal{R}_0$ corresponds to the solid black line in Figure 4. The upper and lower bounds on the reproductive number $\mathcal{R}_0$ given in equations (14) in theorem 4.1 are also illustrated in Figure 4 by the dot-dashed curve and the dashed curve, respectively. In each case, we consider six scenarios where the other basic reproductive numbers are fixed: either both less than one, both greater than one, one greater than one and one less than one, and the various relationships between the two. In particular, the figures labeled **A-F** in figure 4(a) correspond to the following choice of parameters: **A**: $\tau_{AB} = \frac{1}{4} < \frac{3}{4} = \mathcal{R}_{BC} < 1$; **B**: $\mathcal{R}_{BC} = \frac{1}{4} <$

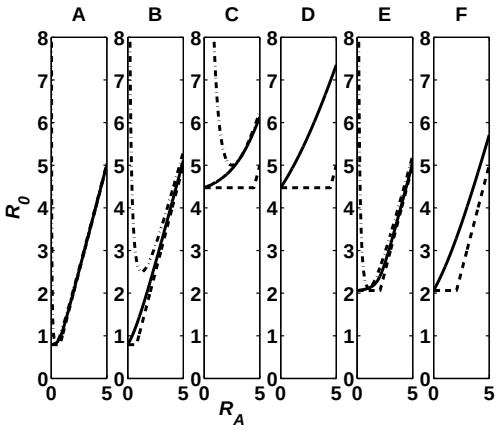

(a) $\mathcal{R}_0$ vs $\mathcal{R}_A$

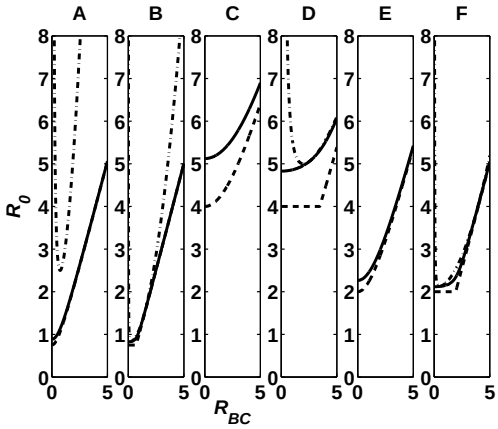

(b) $\mathcal{R}_0$ vs $\mathcal{R}_{BC}$

FIGURE 4. The basic reproductive number of the disease for the three population model, $\mathcal{R}_0$ represented in the solid black curve is illustrated as a function of basic reproductive numbers of the subsystems, $\mathcal{R}_A$ in figure 4(a) and $\mathcal{R}_{BC}$ in figure 4(b). The reproductive number corresponds to the maximum root of the polynomial (13). Also plotted are the upper bounds, indicated with the dot-dashed curve and lower bounds indicated with the dashed curve, defined by equation (14) in theorem 4.1. The figures labeled **A-F** in figure 4(a) correspond to the following choice of parameters: **A**: $\tau_{AB} = \frac{1}{4} < \frac{3}{4} = \mathcal{R}_{BC} < 1$; **B**: $\mathcal{R}_{BC} = \frac{1}{4} < \frac{3}{4} = \tau_{AB} < 1$; **C**: $1 < \tau_{AB} = 2 < 4 = \mathcal{R}_{BC}$; **D**: $1 < \mathcal{R}_{BC} = 2 < 4 = \tau_{AB}$; **E**: $\tau_{AB} = \frac{1}{2} < 1 < 2 = \mathcal{R}_{BC}$; **F**: $\mathcal{R}_{BC} = \frac{1}{2} < 1 < 2 = \tau_{AB}$, and the figures labeled **A-F** in figure 4(b) correspond to the following choice of parameters: **A**: $\mathcal{R}_A = \frac{1}{4} < \frac{3}{4} = \tau_{AB} < 1$; **B**: $\tau_{AB} = \frac{1}{4} < \frac{3}{4} = \mathcal{R}_A < 1$; **C**: $1 < \mathcal{R}_A = 2 < 4 = \tau_{AB}$; **D**: $1 < \tau_{AB} = 2 < 4 = \mathcal{R}_A$; **E**: $\mathcal{R}_A = \frac{1}{2} < 1 < \tau_{AB} = 2$; **F**: $\tau_{AB} = \frac{1}{2} < 1 < 2 = \mathcal{R}_A$.

$\frac{3}{4} = \tau_{AB} =< 1$; **C**: $1 < \tau_{AB} = 2 < 4 = \mathcal{R}_{BC}$; **D**: $1 < \mathcal{R}_{BC} = 2 < 4 = \tau_{AB}$; **E**: $\tau_{AB} = \frac{1}{2} < 1 < 2 = \mathcal{R}_{BC}$; **F**: $\mathcal{R}_{BC} = \frac{1}{2} < 1 < 2 = \tau_{AB}$. A necessary condition for the disease free equilibrium to be locally stable is that $\mathcal{R}_0 < 1$ and the reproductive number $\mathcal{R}_0$ represented by the solid line is only less than one in figures 4(a) **A-B**. We note that Figures 4(a) **A-B** correspond to values of τ_{AB} and $\mathcal{R}_{BC}$ are also less than one, supporting the hypothesis that $\tau_{AB} < 1$ and $\mathcal{R}_{BC} < 1$ are necessary conditions for $\mathcal{R}_0 < 1$.

The parameters for the figures labeled **A-F** in figure 4(b) correspond to the following choice of parameters: **A**: $\mathcal{R}_A = \frac{1}{4} < \frac{3}{4} = \tau_{AB} < 1$; **B**: $\tau_{AB} = \frac{1}{4} < \frac{3}{4} = \mathcal{R}_A < 1$; **C**: $1 < \mathcal{R}_A = 2 < 4 = \tau_{AB}$; **D**: $1 < \tau_{AB} = 2 < 4 = \mathcal{R}_A$; **E**: $\mathcal{R}_A = \frac{1}{2} < 1 < \tau_{AB} = 2$; **F**: $\tau_{AB} = \frac{1}{2} < 1 < 2 = \mathcal{R}_A$. Similar to the results in figure 4(a), the reproductive number $\mathcal{R}_0$ represented by the solid line is only less than one in figures 4(b) **A-B**. These figures also correspond to the only set of parameter values for $\mathcal{R}_A$ and τ_{AB} are less than one, thus also supporting the hypothesis that $\tau_{AB} < 1$ and $\mathcal{R}_{BC} < 1$ are necessary conditions for $\mathcal{R}_0 < 1$.

Figure 4 also demonstrates that the upper and lower bounds given in equations (14) in theorem 4.1 are actually good approximations of the actual reproductive number, even though there was no claim of optimality of the bounds in the theorem. When the decoupled basic reproductive numbers in each of the twelve cases becomes larger, the lower bound becomes a better estimate of the basic reproductive numbers. The dynamics of the basic reproductive numbers reflects the respective intensities of the disease in subpopulations, that is, if the disease increases in intensity in a particular subpopulation, eventually the full system will assume the basic reproductive number of that subpopulation. These values approach the size of the lower bounds $\max\left(\mathcal{R}_A, \sqrt{\tau_{AB}^2 + \mathcal{R}_{BC}^2}\right)$ which are functions of the population that intra-mixes, AB and BC, and the population A with itself. We also note if any of the basic reproductive numbers of the decoupled subsystems are greater than one, this will force the reproductive number $\mathcal{R}_0$ of the entire system to become large. Conversely, a necessary condition for $\mathcal{R}_0$ to be less than one is that the decoupled basic reproductive numbers are also less than one. We note that this occurs only in figures 4(a)(**A**,**B**) and 4(b)(**A**, **B**).

5. **Endemic equilibrium.** In this section, we compute conditions under which the endemic equilibrium exists in the feasible region, as well as bounds on the values of the endemic equilibrium in terms of the basic reproductive number of the subsystems. We note the equilibria are roots of a quartic equation, and thus algebraic solutions are not easily obtained, whereas the basic reproductive number of the subsystems are easily obtainable algebraically.

The equilibria of our system are the steady states of Eqs (3-5). From these algebraic equations, we are able to obtain the following expressions for the endemic equilibrium terms x^* and z^*, in terms of y^*:

$$x^* = \frac{\delta_B y^* \left[\mathcal{R}_{BC}^2 \left(\beta_{CB} + \delta_B\right) y^* - \beta_{CB}\left(\mathcal{R}_{BC}^2 - 1\right)\right]}{\left(\mathcal{R}_{BC}^2 y^* \delta_B + \beta_{CB}\right)\left(1 - y^*\right)\beta_{AB}}, \tag{20}$$

$$z^* = \frac{y^* \beta_{BC}}{y^* \beta_{BC} + \delta_C}, \tag{21}$$

where y^* satisfies

$$y^* = \left\{ y \,\middle|\, \frac{\delta_A \delta_B y\, Q\left(y\right)}{\left(\delta_B y \mathcal{R}_{BC}^2 + \beta_{CB}\right)^2 {\beta_{AB}}^2 \left(y - 1\right)^2} = 0 \right\}, \tag{22}$$

where $Q(y) = b_4y^4 + b_3y^3 + b_2y^2 + b_1y + b_0$ with the coefficients

$$b_4 = \left(\frac{\mathcal{R}_{BC}^2\tau_{AB}\delta_B\beta_{CB}}{\delta_C}\right)^2 (\beta_{AB} + \delta_B + \beta_{CB}), \tag{23}$$

$$b_3 = \left(\frac{\mathcal{R}_{BC}^2\delta_B\beta_{CB}^2}{\delta_C^2}\right)\Big\{\tau_{AB}^2\left[\left(\beta_{CB} - \mathcal{R}_{BC}^2\delta_B\right)\left(\beta_{CB} + 2\beta_{AB} + 2\delta_B\right)\right] \tag{24}$$
$$+ \mathcal{R}_{BC}^2\left[\delta_B\left(\beta_{AB} - \mathcal{R}_A\left(2\beta_{CB} + \beta_{AB} + \delta_B - \beta_{CB}^2\right)\right) + \beta_{AB}\beta_{CB}\left(1 - \mathcal{R}_A\right)\right]\Big\},$$

$$b_2 = \left(\frac{\beta_{CB}}{\delta_C}\right)^2\Big\{\mathcal{R}_{BC}^2\beta_{CB}\left[\mathcal{R}_A\delta_B\left(-2\beta_{CB} - 2\delta_B - 2\beta_{AB}\right) + \beta_{AB}\beta_{CB}(1 - \mathcal{R}_A)\right. \tag{25}$$
$$-\tau_{AB}^2\delta_B\left(2\beta_{CB} + 4 + 2\delta_B\right) + 2\delta_B\beta_{AB}\Big] + \tau_{AB}^2\beta_{CB}^2\left(\beta_{AB} + \delta_B\right)$$
$$+\mathcal{R}_{BC}^4\left[2\mathcal{R}_A\delta_B\left(\beta_{CB}\left(\beta_{CB} + 2\delta_B + 2\beta_{AB}\right) + \delta_B\beta_{AB}\right) + \tau_{AB}^2\delta_B^2\left(\beta_{AB} + \beta_{CB}\right)\right.$$
$$\left.-\delta_B\beta_{AB}\left(2\beta_{CB} + \delta_B\right)\right]\Big\},$$

$$b_1 = \left(\frac{\beta_{CB}^3}{\delta_C^2}\right)\Big\{\mathcal{R}_{BC}^2\left[2\mathcal{R}_A\left(\delta_B\beta_{CB} + \beta_{AB}\beta_{CB} + \delta_B\beta_{AB}\right) - 2\beta_{AB}(\beta_{CB} + \delta_B)\right. \tag{26}$$
$$\left.+\delta_B\tau_{AB}^2(\beta_{CB} + 2\beta_{AB})\right] + (1 - \mathcal{R}_A)\,\beta_{AB}\beta_{CB} + \beta_{CB}\mathcal{R}_A\delta_B$$
$$-\tau_{AB}^2\beta_{CB}(2\beta_{AB} + \delta_B) + \mathcal{R}_{BC}^4\delta_B((1 - \mathcal{R}_A)\beta_{AB} - \beta_{CB}\mathcal{R}_A)\Big\},$$

$$b_0 = \left(\frac{\beta_{AB}\beta_{CB}^4}{\delta_C^2}\right)\left[\tau_{AB}^2(1 - \mathcal{R}_A)(1 - \mathcal{R}_{BC}^2)\right]. \tag{27}$$

Nontrivial steady states y^* are roots of $Q(y)$, thus, there are at most four nontrivial equilibria of our system. Using the Intermediate Value Theorem applied to $Q(y)$, we are able to determine that a value for y^* exists in $(0,1)$ when $\tau_{AB}^2 > (\mathcal{R}_A - 1)\left(\mathcal{R}_{BC}^2 - 1\right)$. For values of $y^* \in (0,1)$, we have to then show that the corresponding values of x^* and z^* are also in (0,1). This will ensure that the endemic equilibrium is in the feasible region $(0,1)\times(0,1)\times(0,1)$. When $y^* \in (0,1)$, then with z^* given by Eq (21), we automatically have $z^* \in (0,1)$. However, x^* does not always lie in the feasible region for all $y^* \in (0,1)$, therefore we must place restrictions on y^* to guarantee that $x^* \in (0,1)$. Using equation (20), we note that the value for x^* is positive when

$$y^* < \frac{\left(\delta_B\mathcal{R}_{BC}^2 + \beta_{CB}\right)\beta_{AB}}{\delta_B\beta_{CB}\left(\mathcal{R}_{BC}^2 - 1\right)}. \tag{28}$$

This requires us to place two conditions on y^*, one for the case where $\mathcal{R}_{BC}^2 < 1$ and one for the case where $\mathcal{R}_{BC}^2 > 1$ to be certain that $x^* \in (0,1)$. In Figure 5, x^* is plotted as a function of y^* with $\mathcal{R}_{BC}^2 < 1$ in Figure 5(a) and with $\mathcal{R}_{BC}^2 > 1$ in Figure 5(b) . For x^* to be in the feasible region, y^* is always bounded above by ξ, but has a differing lower bound depending upon the size of $\mathcal{R}_{BC}$.

The following theorem summarizes the necessary conditions on y^* for the endemic equilibrium to lie within the feasible region. The inequalities in the theorem are obtained by combining the inequality in Eq. (28) and the definition for y^* in Eq. (22).

Theorem 5.1. *The point (x^*, y^*, z^*), satisfying Eqs (20, 22, 21), is an endemic equilibrium of the three population system when $\tau_{AB}^2 > (\mathcal{R}_A - 1)\left(\mathcal{R}_{BC}^2 - 1\right)$ and the following conditions on y^* are satisfied:*

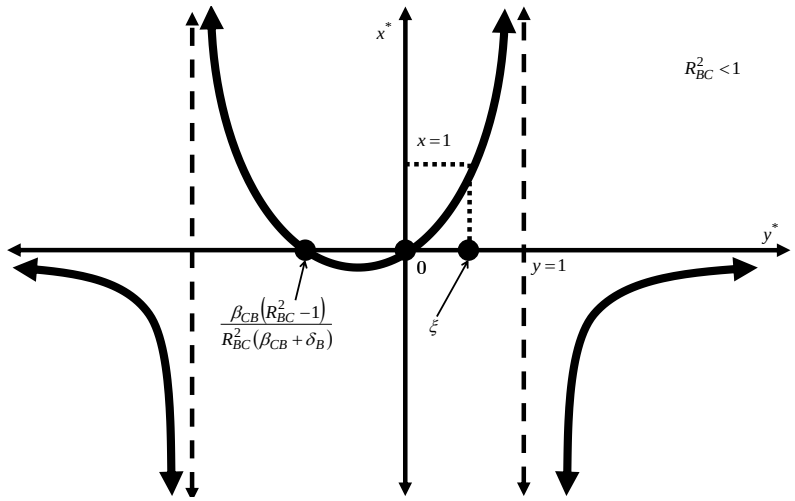

(a) Figure A

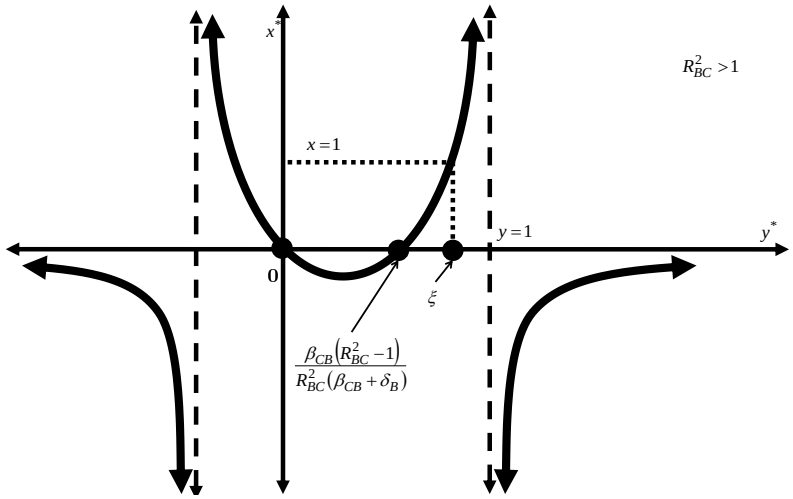

(b) Figure B

FIGURE 5. Bounding x^*. This figure depicts x^* as a function of y^*. In the top figure $\mathcal{R}_{BC}^2 > 1$, then $x^* \in (0,1)$ when $0 < y^* < \xi < 1$. In the bottom figure $\mathcal{R}_{BC}^2 < 1$ then x^* is in $(0,1)$ when $0 < \frac{\beta_{CB}\left(\mathcal{R}_{BC}^2 - 1\right)}{\mathcal{R}_{BC}^2(\beta_{CB}+\delta_B)} < y^* < \xi < 1$.

i. If $\mathcal{R}_{BC}^2 < 1$, *then* $0 < y^* < \xi < 1$,

ii. If $\mathcal{R}_{BC}^2 > 1$, *then* $0 < \frac{\beta_{CB}\left(-1+\mathcal{R}_{BC}^2\right)}{\mathcal{R}_{BC}^2(\beta_{CB}+\delta_B)} < y^* < \xi < 1$,

where, $\xi = \frac{1}{2}\frac{t_1+\sqrt{t_2}}{\delta_B \mathcal{R}_{BC}^2(\delta_B+\beta_{AB}+\beta_{CB})}$ *with* $t_1 = \left(\delta_B \mathcal{R}_{BC}^2 - \beta_{CB}\right)\beta_{AB} + \delta_B\beta_{CB}\left(\mathcal{R}_{BC}^2 - 1\right)$ *and* $t_2 = \left(\delta_B \mathcal{R}_{BC}^2 + \beta_{CB}\right)^2 {\beta_{AB}}^2 + 2\beta_{CB}\delta_B\left(\mathcal{R}_{BC}^2 + 1\right)\left(\delta_B \mathcal{R}_{BC}^2 + \beta_{CB}\right)\beta_{AB} + {\delta_B}^2{\beta_{CB}}^2 \left(\mathcal{R}_{BC}^2 - 1\right)^2$.

Thus using we have established conditions for which the endemic equilibrium exists and lies in the feasible region. Lajmanovich and Yorke [27, Lemma 3.2, p. 226] also establish existence results and provide conditions on the stability of the endemic equilibrium equivalent to those given in Proposition 1 [27, Theorem 3.1, p. 227], but do not provide estimates on the endemic equilibrium in terms of computable quantities such as basic reproductive numbers of the subsystems.

Figure 6 displays the dynamics of the full system (x, y, z) over time with ten randomly selected initial conditions. The shaded gray areas represent the bounds for y^* found in Theorem 5.1. Figure 6(b) contains an enlarged version of the figure displaying the behavior of y. For both Figure 6(a), corresponding to $\mathcal{R}_{BC} < 1$, and Figure 6(b), corresponding to $\mathcal{R}_{BC} > 1$, we see the value of the y-component of the endemic equilibrium is within the bounds given in Theorem 5.1. The trajectories converge to the endemic equilibrium of the full system for both the initial conditions shown in the figure and many other simulations (not shown here). Our numerical results suggest that the endemic equilibrium of the full system is globally asymptotically stable provided the conditions in Theorem 5.1 hold.

6. **Alternate model for the full system.** Thus far, we have studied the benefit of decompartmentalizing the full system into decoupled subsystems in order to get a sense of the dynamics of the full system. The basic reproductive numbers of the disease in the decoupled subsystems has allowed us to obtain upper and lower bounds for the basic reproductive number in the full system. Also, we are able to use these expressions to decrease the impact of the infection transmission between populations A and B. In this section, we provide an *alternate* approach to studying the dynamics of the full system. We develop an alternate formulation of the full system in which the connections between System I and System II are replaced with nonhomogeneous constant forcing terms. We will use the values of the globally asymptotically stable endemic equilibria of the decoupled subsystems (Eqs. (7) and (9)) to represent an influx of disease between populations A and B, as depicted in Figure 7. Recall the motivation behind the interactions within the model: the spread of a sexually transmitted disease within heterosexual females, heterosexual males, and bisexual males. The influx terms represent an inflow of disease contraction within the heterosexual female and bisexual male populations. The advantages of this alternate formulation of the full system include an explicit representation of the endemic equilibrium. This formulation also provides a comparison between the dynamics of the subpopulations and the dynamics of the full system. In addition we will show the dynamics of this alternate formulation given in Eqs. (29 - 31) provide a close approximation to the dynamics of the full system given in Eqs. (3 - 5).

In Figure 7 we illustrate how the dynamics of one system influences the dynamics of the other. The solid arrows represent the interactions between the subpopulations and the dashed arrows labeled by f and g represent the influence between populations A and B modeled as nonhomogeneous forcing terms. The term forcing here is used in a physics or mathematical context, where an external nonhomogeneous term is added to a homogeneous system. In this context, the external force of the constant influx of infection, f and g, pushes the equilibrium of the system away from the disease free equilibrium. Note that while disease influx rates between systems I and II are constant, the incidence rate $d(x + y + z)/dt$, the number of new cases per population at risk in a given time period, is variable. The equations representing these interactions remain decoupled as seen in

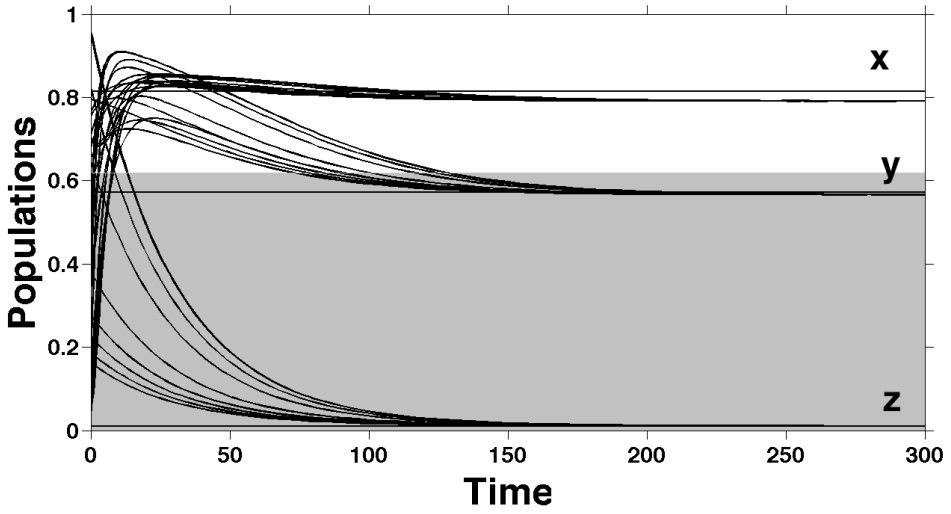

(a) x, y, z vs Time. $\mathcal{R}_{BC} < 1$

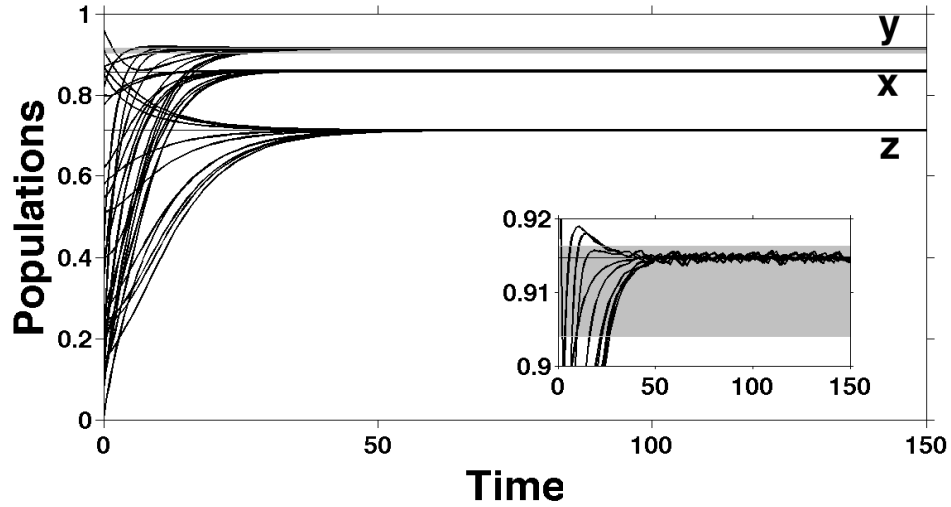

(b) x, y, z vs Time. $\mathcal{R}_{BC} > 1$

FIGURE 6. The figures display the dynamics of the full (x, y, z) system over time with randomly selected initial conditions. The shaded gray areas represent the bounds for y^* found in Theorem 5.1. In figure 6(a), $\mathcal{R}_{BC}$ is less than one, and $\mathcal{R}_{BC}$ is greater than one in figure 6(b). Figure 6(b) contains an enlarged version of the figure displaying the behavior of y. Parameters are as listed in Table 2 correspond to $\beta_{AA} = 0.7368$, $\beta_{AB} = 0.4911$, $\beta_{BA} = 0.1491$, $\beta_{CB} = 0.13419$, and $\delta_A = \delta_B = \delta_C = 0.1$. In 6(a) $\beta_{BC} = 0.1863$ which gives $\mathcal{R}_{BC} = 0.5$ and in 6(b) $\beta_{BC} = 26.8$ which gives $\mathcal{R}_{BC} = 6$. This large value of $\mathcal{R}_{BC}$ was chosen to easily distinguish the endemic equilibrium values for x, y, and z.

$$\frac{dx}{dt} = (\beta_{AA}x + g)(1-x) - \delta_A x, \tag{29}$$

$$\frac{dy}{dt} = (\beta_{CB}z + f)(1-y) - \delta_B y, \tag{30}$$

$$\frac{dz}{dt} = \beta_{BC}y(1-z) - \delta_C z, \tag{31}$$

where $f = \beta_{AB}{x_1}^*$ and $g = \beta_{BA}y_2^*$ with x_1^* as defined in Eq. (7) and y_2^* as defined in Eq (9). We can compare system III shown in Figure 7 to that in Figure 2 and see that the dashed lines representing our forcing terms f and g simulate the direct connection between populations A and B shown with the solid lines and given respectively by $\beta_{AB}x_1^*$ and $\beta_{BA}y_3^*$. The system of differential equations given in Eqs. (29-31) have replaced the direct connection terms in Eqs. (3-5) with the forcing terms f and g which decouples the system of three equations, but still retains the effect of input of disease between populations A and B, albeit at a constant rate dependent on the endemic equilibrium value of the influencing population. Thus system III is an intermediate model between the completely decoupled systems I and II and the fully connected model.

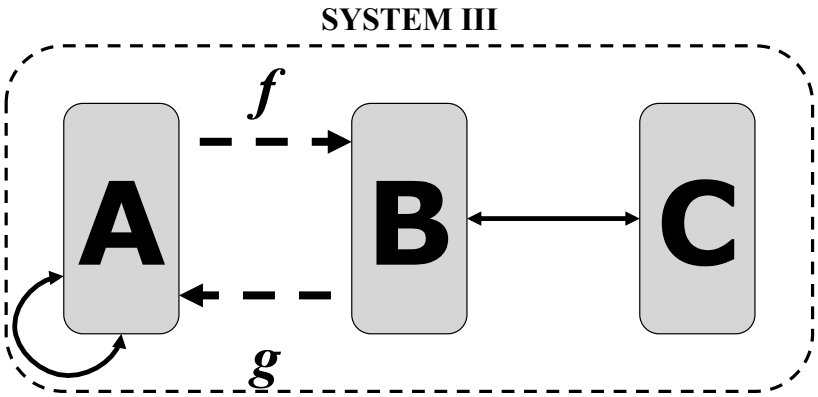

FIGURE 7. Deconstructed Model with Nonhomogeneous Forcing Terms: f is a function of the endemic equilibrium of System I, x_1^*, and g is a function of one term of the endemic equilibrium of System II, y_2^*.

There is no longer a disease-free equilibrium in System III since there is a constant influx of disease from population A into B and B into A. As a result, the disease always persists in the population when there is a constant influx of disease between population A, bisexual males in our motivational example, and B, heterosexual females in our example. This idea may seem obvious: if you are constantly inserting infectives into a population then the disease will not have an opportunity to die out. Perhaps the model with *influence terms* is a more realistic representation of the dynamics of the disease considering that it is indeed incurable and there may never be a case when the disease is completely eradicated from the population. Consider, for example, our motivational example with incurable sexually transmitted disease

in the male bisexual, female heterosexual, and male heterosexual populations. The disease may not be eradicated due to inadequate access to healthcare, persistent homophobia, and a number of other sociological and epidemiological factors. The next proposition shows that the endemic equilibrium is locally asymptotically stable.

Proposition 2. *The Endemic Equilibrium*

$$(x_3^*, y_3^*, z_3^*) = \left(\frac{\eta_4 + \sqrt{\eta_4^2 + 4\beta_{AA} g}}{2\beta_{AA}}, \frac{-\eta_1 + \eta_3}{2\eta_2}, \frac{\beta_{BC}(\eta_1 - \eta_3)}{\beta_{BC}(\eta_1 - \eta_3) - 2\delta_C \eta_2} \right), \tag{32}$$

where:

$$\eta_4 = -g + \beta_{AA} - \delta_A, \tag{33}$$

$$\eta_3 = \sqrt{\eta_1^2 - 4\eta_2 \eta_0}, \tag{34}$$

$$\eta_2 = \beta_{BC}(f + \beta_{CB} + \delta_B), \tag{35}$$

$$\eta_1 = \delta_C(f + \delta_B - \mathcal{R}_{BC}\delta_B) - f\beta_{BC}, \tag{36}$$

$$\eta_0 = -\delta_C f. \tag{37}$$

exists, is unique, and is locally asymptotically stable.

Proof. Note the dynamics of x, see Eq (29), are completely decoupled from that of y and z in Eqs (30, 31). Hence the first component, x_3^* in Eq. (32) comes solely from solving for the equilibrium in Eq (29). The second two components, (y_3^*, z_3^*), in Eq (32) come from solving for equilibrium in Eqs (30, 31). The second two components of the equilibrium in Eq (32) reduce to the disease-free equilibrium for the unforced System II, i.e. Eqs (4, 5), as $f \to 0$, and the endemic equilibrium for the unforced System II, (y_2^*, z_2^*), moves outside the domain $[0,1] \times [0,1]$ for $f > 0$.

Next we show x_3^* lies in the domain $[0,1]$ for $g \geq 0$. Since $\beta_{AA} > 0$ then $x_3^* \geq 0$. Since there is no disease-free equilibrium, there is no basic reproductive number for System I with $g > 0$. However, we define a basic reproductive-like number

$$\tilde{\mathcal{R}}_A(g) = \beta_{AA}/(g + \delta_A), \tag{38}$$

which comes from performing the Next Generation method evaluated at $x_3 = 0$ for Eq. (29) alone. Note this expression is a definition of a certain combination of parameters that will be important for our analysis below, but since it is not a basic reproductive number is the true sense, it cannot be used to draw stability conclusions based on the Next Generation Method, particularly since there is no disease-free equilibrium.

In the case when g is zero, we are returned to system I with $\tilde{\mathcal{R}}_A(0) = \mathcal{R}_A$. With this basic reproductive-like number $\tilde{\mathcal{R}}_A(g)$ we can rewrite x_3^* as:

$$\begin{aligned} x_3^* &= \frac{(\tilde{\mathcal{R}}_A(g) - 1) + \sqrt{(\tilde{\mathcal{R}}_A(g) - 1)^2 + \frac{4g\tilde{\mathcal{R}}_A^2(g)}{\beta_{AA}}}}{2\tilde{\mathcal{R}}_A(g)}, \\ &= \frac{1}{2}\left(1 - \frac{1}{\tilde{\mathcal{R}}_A(g)}\right) + \sqrt{\frac{1}{4}\left(1 - \frac{1}{\tilde{\mathcal{R}}_A(g)}\right)^2 + \frac{g}{\beta_{AA}}}, \\ &< \frac{1}{2}\left(1 - \frac{1}{\tilde{\mathcal{R}}_A(g)}\right) + \sqrt{\frac{1}{4}\left(1 - \frac{1}{\tilde{\mathcal{R}}_A(g)}\right)^2 + \frac{1}{\tilde{\mathcal{R}}_A(g)}}, \\ &< \frac{1}{2}\left(1 - \frac{1}{\tilde{\mathcal{R}}_A(g)}\right) + \sqrt{\frac{1}{4}\left(1 + \frac{1}{\tilde{\mathcal{R}}_A(g)}\right)^2} = 1, \end{aligned} \tag{39}$$

as $\tilde{\mathcal{R}}_A(g) < \beta_{AA}/g$. Thus $x_3^* \in (0,1)$. The equilibria for the second two components in Eq (32) are non-trivial equilibrium points. We identify the right hand sides of Eqs. (30) and (31) as $\mathbf{F}_2(y,z)$ and $\mathbf{F}_3(y,z)$ respectively. Note that $\mathbf{F}_2(0,z) = f+\beta_{CB}z > 0$ and $\mathbf{F}_2(1,z) = -\delta_B$. Similarly $\mathbf{F}_3(y,0) = \beta_{BC}y > 0$ and $\mathbf{F}_3(y,1) = -\delta_C$. We can consider z in $\mathbf{F}_2$ and y in $\mathbf{F}_3$ as fixed and apply the Intermediate Value Theorem. The sign changes of the functions of both $\mathbf{F}_2$ and $\mathbf{F}_3$ assures us that we have at least one endemic equilibria. The sign of η_1 defined in Eq (36) is not intrinsic but depends on the size of the disease removal rates, infection influence, and the external force f. However, we note that in any case, $\eta_1^2 - 4\eta_2\eta_0 > 0$ (because of the signs of η_2 and η_0) which implies $\eta_3 > \eta_1$. Thus, we now see that $-\eta_1 + \eta_3 > 0$. The other equilibrium solution that arises from the solution of Eqs (30) and (31) lies outside of the $(0,1)$ interval. As a result, (y_3^*, z_3^*), defined in Eq (32) is the only equilibrium that lies within $(0,1)$. Thus, the endemic equilibrium exists in the feasible region and is unique.

Next we explore the local stability of the endemic equilibrium. Since the equations are decoupled, we first look at the stability of x_3^*. In order to show the first component is locally asymptotically stable for Eq (7) we need to show the eigenvalue of the Jacobian, $\lambda = \beta_{AA}(1-2x_3^*) - \delta_A - g$ for this equation is negative. This is equivalent to requiring $x_3^* > \eta_4/2\beta_{AA}$ which is clearly satisfied by the definition of x_3^* in Eq (32).

In order to show the y_3^* and z_3^* components of the endemic equilibrium in Eq (32) are asymptotically stable for the dynamics defined by Eqs (30, 31), one must evaluate the Jacobian of the vector field at the endemic equilibrium and show the trace is negative and the determinant is positive. The trace $-(\delta_B+\delta_C+f+\beta_{BC}y_3^*+\beta_{CB}z_3^*)$ is clearly negative. We recognize the definition of z_3^* from Eq (32) may be written in terms of y_3^* as

$$z_3^* = \frac{\beta_{CB}y_3^*}{\beta_{CB}y_3^* + \delta_C}. \tag{40}$$

We substitute this expression for z_3^* into the determinant of the Jacobian

$$\begin{aligned} & 1 + \mathcal{R}_{BC}(y_3^* + z_3^* - 1) + \frac{\beta_{BC}}{\delta_C}\left(y_3^* + \frac{f}{\delta_B}\right) + \frac{1}{\delta_B}\left(f + \beta_{CB}z_3^*\right), \qquad (41) \\ = \; & \frac{\eta_1\delta_C + \beta_{BC}^2 y_3^*\left((\beta_{CB}+f)(1+y_3^*) + \delta_B y_3^*\right)}{\delta_C + \beta_{BC}y_3^*} + \\ & + \frac{\beta_{BC}\left(\eta_1 y_3^* + \delta_C\left(f(1+y_3^*) + y_3^*(2\beta_{CB}+\delta_B)\right)\right)}{\delta_C + \beta_{BC}y_3^*} > 0, \end{aligned}$$

thereby showing the determinant is positive and the endemic equilibrium is therefore locally asymptotically stable. □

Proposition 3. *The Endemic Equilibrium (x_3^*, y_3^*, z_3^*) is globally asymptotically stable.*

Proof. Since the system is actually decoupled with the influence terms, we need only to look at x_3^* and then (y_3^*, z_3^*) separately. Identifying the right hand side of Eq. (29) as the function $h(x)$, we note that in one-dimension, to extend local asymptotic stability to global asymptotic stability $h(x)$ requires the condition, $|h(x)| > 0$ for all $x \in (0,1)$ and $x \neq x_3^*$. We have shown that $h(x) = 0$ only at the unique the equilibrium, $x = x_3^*$, so x_3^* is globally asymptotically stable [17, 46].

The goal of this proof for (y_3^*, z_3^*) is to show the trajectories with initial values in the domain of our problem converge to the endemic equilibrium point. In order to

show this for our unique (y_3^*, z_3^*) we must first show there exists a compact absorbing set in $[0,1] \times [0,1]$. Then we can apply Poincaré-Bendixson's criterion $div\mathbf{F} < 0$ for $\mathbf{V}' = \mathbf{F}(\mathbf{V})$ to show that the system has no periodic orbits and the endemic equilibria is globally stable in $[0,1] \times [0,1]$.

We define a square absorbing set $K = [0,1] \times [0,1]$, where K is connected since it is a convex subset of $\mathbb{R}$ with the non-trivial endemic equilibrium (y_3^*, z_3^*) given by Eq. (32) in the interior. Any orbit with initial condition in K must remain in K since the vector field points inward along the boundary of K[1] and by the Poincaré -Bendixson theorem, approach either the unique endemic equilibrium (y_3^*, z_3^*) or a periodic orbit. Since $divF = -(\beta_{CB} z_3 + f + \delta_B + \beta_{BC} y_3 + \delta_C)$ is negative for all values of $(y_3, z_3) \in K$, there are no periodic orbits in K, and all orbit must approach the unique endemic equilibrium (y_3^*, z_3^*) . Hence, (x_3^*, y_3^*, z_3^*) is globally asymptotically stable. □

7. **Example: Application to HIV.** Sexually transmitted diseases can be characterized as either viral, such as herpes, HPV, and HIV, or bacterial, such as chlamydia, gonorrhea and syphilis. In general bacterial STDs are curable by antibiotics, whereas viral STDs are not. Malaria models such as [52] inspired early models of STDs such as [13, 27]. Mathematical modeling in the area of sexually transmitted diseases shifted towards incurable diseases during the 1980's with the emergence of the HIV/AIDS epidemic (see for example [1, 8, 2, 20, 21, 22, 23, 58]).

The introduction of highly active antiretroviral therapy (HAART), a treatment paradigm utilizing three or more antiretroviral drugs in combination, has led to a significant decrease in HIV-associated morbidity and mortality [14]. In more developed countries with ready access to highly active antiretrovial therapy (HAART), the progression to AIDS has dropped drastically [14, 42, 43, 55]. Studies of the life expectancy of individuals treated with combination antiretroviral therapy [4, 12, 37, 38, 42, 43, 47, 50, 53, 55] show that access to antiretroviral therapy has improved life expectancy to the extent that HIV is increasingly considered as a chronic illness. For example, a life expectancy of 40-50 additional years after contracting HIV at age 20 corresponds to a range of μ_j between 0.0018 to 0.003 [34, 42, 57]. Thus with the introduction of HAART therapies, the values of μ for HIV is small. In Figure 8, we compare population sizes for each of the three subpopulations A, B,C, as μ varies from 0 to 0.01, corresponding to the values of μ for HIV with HAART therapy. In Figures 8, 9, and 10 we are using the parameter values detailed in Table 2 taken from various HIV studies [39], [48].

In this application, we examine the spread of HIV within a population consisting of homosexual interactions within a bisexually mixing male population as well as heterosexual couplings between males and females. Recall, population A corresponds to bisexual males, population B depicts heterosexual females, and population C represents heterosexual males. Figure 8 demonstrates that solutions for μ small approach the solution corresponding to $\mu = 0$. The long term dynamics of each of the scaled proportion of individuals infected in the respective subpopulations of the full system, $I_A \Lambda d_A / p_A$, $I_B \Lambda d_B / p_B$, and $I_C \Lambda d_C / p_C$ with a small positive μ_j, approach the dynamics of $\mu_j = 0$. The values of μ_j shown in Figure 8 correspond to $\mu_j = 0$ .005, and 0.01. For population A, population B, population C, depicted by the solid, dashed, and dashed-dotted lines in Figure 8, the solution corresponding to

[1]The values $\left(\frac{f}{\delta_B + f}, 0\right)$ with $\frac{dy}{dt} = 0$ and $\left(1, \frac{\beta_{BC}}{\beta_{BC} + \delta_C}\right)$ with $\frac{dz}{dt} = 0$ are not equilibria in our system but rather values where the individual populations reach steady state.

TABLE 2. Parameter Estimates.

Symbol	Description	Value	Reference
(x, y, z)	Initial Conditions	$\frac{25}{100}, \frac{50}{400}, \frac{25}{300}$	[39]
N	Total population	900	[39]
N_B	Total population of B	$\frac{N}{2}$	[39]
N_{AC}	Total population of A and C	$\frac{N}{2}$	[39]
N_C	Total population of C	$N_{AC} \cdot .9$	[39]
N_A	Total population of A	$N_{AC} \cdot .1$	[39]
b_{AA}, $b_{AB} = b_{CB}$, $b_{BA} = b_{BC}$	Probability of infection per exposure in population i to an individual in population j	0.2456, 0.1637, 0.0497	[39]
c_{ij}	Contact number of an individual in population i with a new individual in population j.	Average 3/year	[48], [39]
μ_A, μ_B, μ_C	Death rate due to disease of individuals in population j	$\frac{1}{15}$	[48]
$\frac{1}{d_A}, \frac{1}{d_B}, \frac{1}{d_C}$	Average duration of acquisition of sexual partners	30, 30, 30	[48]

$\mu = 0$ is the top most solution. The middle solution curve for each of the respective populations correspond to $\mu = 0.005$, and the bottom solution curve corresponds to $\mu = 0.01$. Both of these nonzero values of μ_j values overestimate the range of 0.0018 to 0.003 corresponding to previously mentioned HIV life expectancy results [34, 42, 57]. However, the curves corresponding to the values of $\mu_j = 0.0018$ and 0.003 are nearly indistinguishable from the curve for $\mu_j = 0$. Hence we have exaggerated the value of μ_j to illustrate the effect of an increasing μ_j. For all the values of μ_j, the trajectories approach the value of the endemic equilibrium.

Figures 9 and 10 illustrate the connection between the full system and the alternate system by comparing values of the endemic equilibrium, as a function of basic reproductive numbers $\mathcal{R}_A$ and $\mathcal{R}_{BC}$, and also comparing trajectories of both systems, starting with the same initial conditions. First, we compare the dynamics of the full system for the case of HIV given Eqs. (3 - 5) to the alternative formulation given in Eqs. (29 - 31). In particular we will compare the value of the endemic equilibria of the full system (3 - 5) to the value of the endemic equilibria of the alternate system (29 - 31). Figure 9 illustrates the equilibria of both the full system and the alternate system as $\mathcal{R}_A$ and $\mathcal{R}_{BC}$ vary. In particular, Figure 9(a) plots the value of the components of the endemic equilibrium as β_{AA} varies in (6) and Figure 9(b) plots of the value of the components of the endemic equilibrium as β_{CB} varies, with fixed β_{BC} in (8). Figure 9(a) shows the values endemic equilibria of the full system (x^*, y^*, z^*) and the values of the endemic equilibria of the alternate system (x_3^*, y_3^*, z_3^*), as the reproductive number $\mathcal{R}_A$ varies. In each of the components, the values of the components of the endemic equilibria of the alternate system, denoted by the dashed line, gives a good approximation of the values of the components of the endemic equilibria of the full system, denoted by the solid dots. Similar results can be seen in Figure 9(b), as the reproductive number $\mathcal{R}_{BC}$ varies.

These figures illustrate the validity of using the simpler alternate model to understand the behavior of the full system. The simulation results in Figure 9 show that the values of the endemic equilibrium are very similar between the direct and

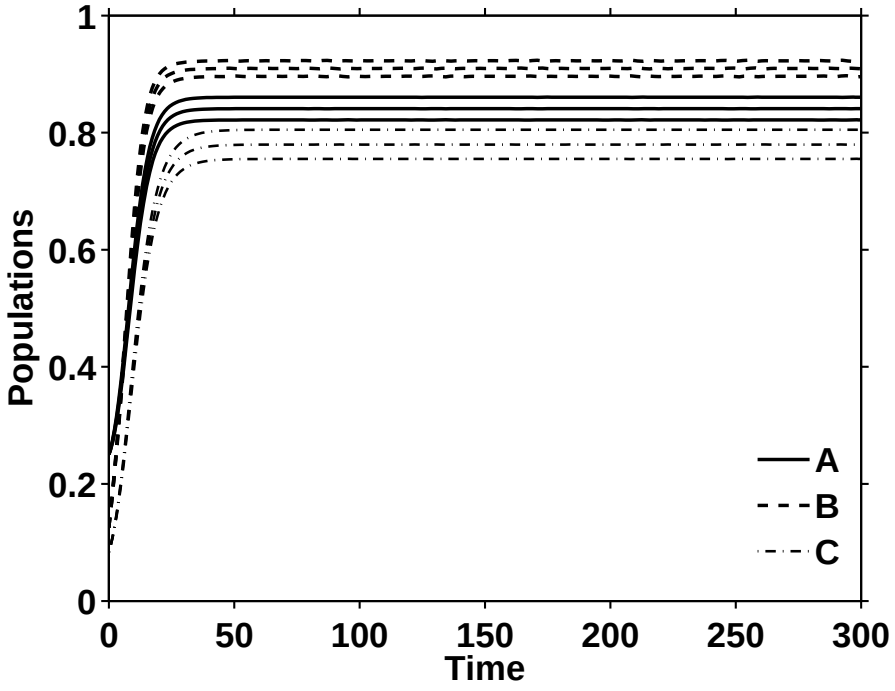

FIGURE 8. The figure displays the dynamics of the scaled proportion of individuals infected in the respective subpopulations of the full system Eqs. (3-5), $I_A\Lambda d_A/p_A$, $I_B\Lambda d_B/p_B$, and $I_C\Lambda d_C/p_C$ versus time as μ_j is varied from 0 to 0.01. Increasing μ_j lowers each population curve: from top to bottom $\mu = 0$, $\mu = .005$, and $\mu = .01$. Parameters are as listed in Table 2 correspond to $\beta_{AA} = 0.7368$, $\beta_{AB} = 0.4911$, $\beta_{BA} = 0.1491$, $\beta_{CB} = 0.13419$, and $\delta_A = \delta_B = \delta_C = 0.1$.

indirect system and Figure 10 shows that the alternate system tracks the full system, as a function of time. Thus, we have numerically demonstrated using both the endemic equilibrium and the basic reproductive numbers that the alternate and algebraically simpler model follows the dynamics and behavior of the full system.

Finally, we can bound the basic reproductive number of the disease in the direct transmission model, $\mathcal{R}_0$, the basic reproductive number for Eqs (3 - 5), in terms of basic reproductive-like numbers from the influenced system, $\tilde{\mathcal{R}}_A(g)$ as defined in Eq. (38) and

$$\tilde{\mathcal{R}}_{BC}(f) = \sqrt{\frac{\beta_{BC}\beta_{CB}}{(f+\delta_B)\delta_C}}. \tag{42}$$

This is described in the theorem below:

Theorem 7.1. *The basic reproductive number $\mathcal{R}_0$ is bounded below by the functions $\tilde{\mathcal{R}}_A(g)$ and $\tilde{\mathcal{R}}_{BC}(f)$.*

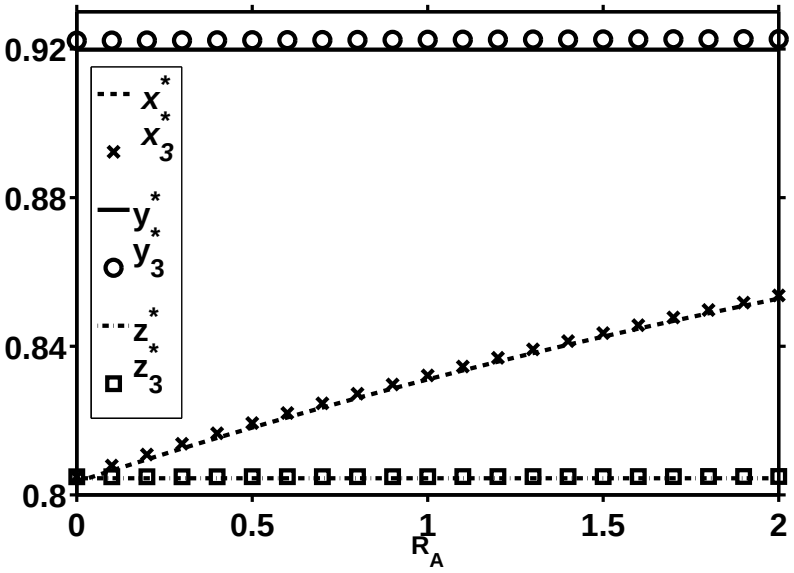

(a) x^*, x_3^*, y^*, y_3^*, z^*, z_3^* vs $\mathcal{R}_A$

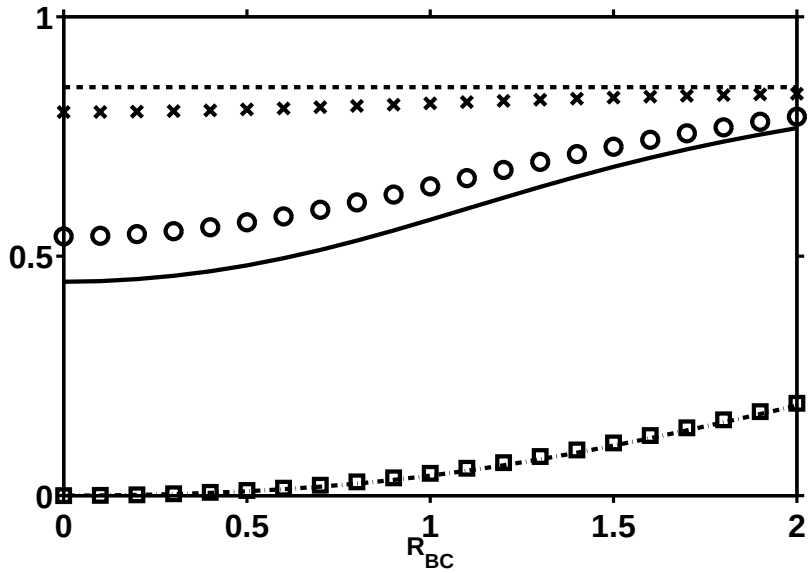

(b) x^*, x_3^*, y^*, y_3^*, z^*, z_3^* vs $\mathcal{R}_{BC}$

FIGURE 9. The figures display the endemic equilibria of the full system (x^*, y^*, z^*), denoted by the solid dots in the figure, and alternate system (x_3^*, y_3^*, z_3^*), as specified in the legend which applies to 9(a) and 9(b), varied with respect to the decoupled basic reproductive numbers $\mathcal{R}_A$ and $\mathcal{R}_{BC}$. Parameters are as listed in Table 2 correspond to $\beta_{AA} = 0.7368$, $\beta_{AB} = 0.4911$, $\beta_{BA} = 0.1491$, $\beta_{CB} = 0.13419$, and $\delta_A = \delta_B = \delta_C = 0.1$. Note that β_{AA} is varying in Figure 9(a), and β_{CB} is varying in Figure 9(b).

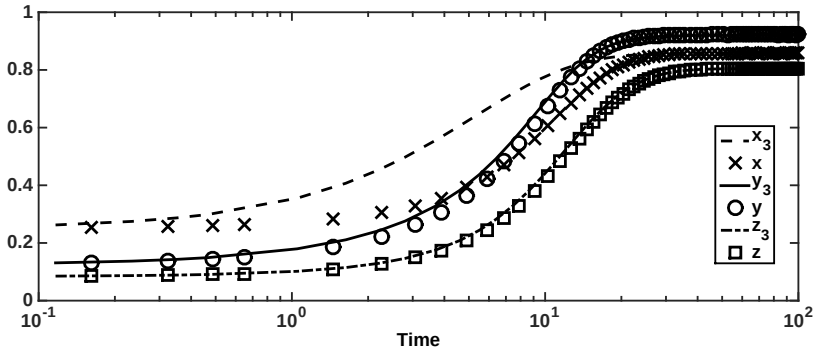

FIGURE 10. Semilogarithmic plot of the alternate (x_3, y_3, z_3) and full (x, y, z) systems over time beginning with the same initial conditions. The alternate system captures the behavior of the full system at the endemic equilibrium. The behavior of the alternate system for populations B and C over short and long the periods matches the full system. The behavior of population A differs initially, with an overestimate on the the part of the alternate system, but both systems converge in the long term. Parameters are as listed in Table 2 correspond to $\beta_{AA} = 0.7368$, $\beta_{AB} = 0.4911$, $\beta_{BA} = 0.1491$, $\beta_{CB} = 0.13419$, and $\delta_A = \delta_B = \delta_C = 0.1$.

Proof. For f and g positive then $\tilde{\mathcal{R}}_A(g) < \mathcal{R}_A$ and $\tilde{\mathcal{R}}_{BC}(f) < \mathcal{R}_{BC}$. In section 4 we established that $\mathcal{R}_0$ is greater than $\mathcal{R}_A$ and $\mathcal{R}_{BC}$, hence it must be bounded below by $\tilde{\mathcal{R}}_A(g)$ and $\tilde{\mathcal{R}}_{BC}(f)$ as well. □

8. **Discussion.** In this paper we consider an epidemiological model of a chronic disease with multiple connections between subpopulations. Motivated by the algebraically intractable basic reproductive numbers and endemic equilibria of this system, we have provided two alternative approaches that not only approximate the dynamics of the full system but also bound the basic reproductive number of the full system. In particular, we provide explicit bounds on the basic reproductive number of the full system in terms the basic reproductive numbers of the smaller subsystems. We introduce an alternate system in which the values of the basic reproductive numbers of the subsystems provide a constant stream of disease into the separate subsystems. The dynamics of the alternative formulation approximates the dynamics of the full system. The basic reproductive-like numbers of the alternate system provide lower bounds on the basic reproductive number of the full system. Providing computationally tractable bounds on the basic reproductive number and value of the endemic equilibrium allows us to study the effect of the subpopulations on the entire population.

With this new method we are able to demonstrate that bridging interactions between mutually exclusive populations effect the prevalence of the disease within the subsystems and ultimately the disease level of the entire system. For example, the interaction number representing the connection between the populations in subsystems I and II is an important part of the upper bound for the basic reproductive number of the full system. By providing tools for analysis of the full populations in

terms of the subpopulations we can target control of the disease rather than eradication. In the case of chronic sexually transmitted diseases, control of the spread of the disease is a realistic goal. In the case of our motivational model, there is not reliable data on the bisexual male population, population A, however our model allows us to understand the effect this population has on the heterosexually mixing populations, B and C.

In our quest to describe the reproduction numbers and endemic equilibrium of the full system, we considered using reproduction invasion numbers in addition to the reproduction and interaction numbers of the subpopulations. Typically invasion reproductive numbers are used in the study of two competing strains of infection. These invasion reproductive numbers quantify the possibility of "invasion" by one strain in an environment in which the other strain is at a positive equilibrium. However, in this case, there is only one strain of infection, and invasion refers to either the infection in system I spilling over into system II, or the infection in system II spilling into system I, through bridging interactions. Invasion reproductive numbers are calculated by evaluating the Jacobian at the boundary equilibrium. For the boundary equilibrium where the infection exists only in system I, $\mathcal{E}_I = \left(\frac{\mathcal{R}_A-1}{\mathcal{R}_A}, 0, 0\right)$ is the endemic equilibrium of the system I given in Eq. (7). The invasion reproductive number $\mathcal{R}_A^{II}$ is then the largest positive eigenvalue of the polynomial

$$\begin{aligned} P_A^{II} &= -\lambda^3 + \left(\mathcal{R}_A^2 + \mathcal{R}_A(\mathcal{R}_A-1)\left[\frac{\beta_{AB}}{\delta_B} - \tau_{AB}^2\right]\right)\lambda^2 + \\ &\left(\frac{(U\mathcal{R}_{BC}^2 + \tau_{AB}^2)\mathcal{R}_A}{UV}\right)\lambda - \frac{\mathcal{R}_{BC}^2\mathcal{R}_A^2\left[(\mathcal{R}_A-1)\frac{\beta_{AB}}{\delta_B} + \mathcal{R}_A\right]}{UV^2}, \end{aligned}$$

where $U = 2\mathcal{R}_A - 1$ and $V = \mathcal{R}_A + (\mathcal{R}_A - 1)\beta_{AB}/\delta_B$. This expression is analytically as intractable as the reproductive number of the full system described the roots of equation (13). The invasion reproduction number $\mathcal{R}_A^{II}$ for an infection in system II spilling into system I is more complicated than a the case of an infection type II invading a population with infection type I as in [9, 44, 49], among many other papers, because of the self interaction of population A with itself (a result of our motivating sexually transmitting disease model with population A representing male bisexuals). Similarly, the invasion reproduction number for an infection from system I invading system II at the boundary equilibrium $\mathcal{E}_{II} = \left(0, \frac{\mathcal{R}_{BC}^2-1}{\mathcal{R}_{BC}^2 - \frac{\beta_{BC}}{\delta_C}}, \frac{\mathcal{R}_{BC}^2-1}{\mathcal{R}_{BC}^2 - \frac{\beta_{CB}}{\delta_B}}\right)$, reflecting the endemic equilibria of the system I given in Eq. (9), is not simple to express analytically. Hence, we chose to use only the reproduction and interaction numbers of the subsystems to bound the basic reproductive number for the full system and to describe the endemic equilibrium of the full system.

The epidemiological impact of this study allows us to target the behavior of population A. Specifically, if intervention strategies, such as targeted sex education, are employed on the members of population A, the disease will die out. In this model, in particular, a bridge exists between a population that intermixes, A, and the cross mixing populations, B and C. This connection is quantified through the manner in which the basic reproductive numbers of System I and System II are linked together by the interaction number τ_{AB}. The population A is the most sexually-interactive in the system given they have the highest number of couplings between groups. Our study shows if their risky interactions with population B

decreases, the disease has the potential to die out within the entire system. We urge public health officials to create a public health campaign to encourage members of population A to either eliminate risky interactions with population B, or take significant protective actions when involved with sexual activities with members of this population.

Acknowledgments. We would like to thank Carlos Castillo-Chavez, Zhilan Feng, and Joseph Previte for their valuable comments and suggestions. KFG acknowledges partial support by a grant from the Simons Foundation (#245237) and NSF grant 1361209.

REFERENCES

[1] R. M. Anderson and R. M. May, *Infectious Diseases of Humans: Dynamics and Control*, Oxford Science Publications, 1991.
[2] N. T. Bailey, Application of stochastic epidemic modelling in the public health control of HIV/AIDS, *Lecture Notes in Biomathematics*, **86** (1990), 14–20.
[3] R. J. Beverton and S. J. Holt, The theory of fishing, in *Sea Fisheries: Their Investigation in the United Kingdom* (ed. M. Graham), Edward Arnold, London, (1956), 372–441.
[4] F. Bonnet, P. Morlat, G. Chene, P. Mercie, D. Neau, M. Chossat, I. Decoin, F. Djossou, J. Beylot, F. Dabis and Groupe d'Epidemiologie Clinique du SIDA en Aquitaine (GECSA), Causes of death among HIV-infected patients in the era of highly active antiretroviral therapy, Bordeaux, France, 1998-1999, *HIV Med.*, **3** (2002), 195–199.
[5] F. Brauer and C. Castillo-Chavez, *Mathematical Models in Population Biology and Epidemiology*, 2^{nd} edition, Springer, New York, 2012.
[6] C. Castillo-Chavez and B. Li, Spatial spread of sexually transmitted diseases within susceptible populations at demographic steady state, *Mathematical Biosciences and Engineering*, **5** (2008), 713–727.
[7] C. Castillo-Chavez, Z. Feng and W. Huang, On the computation $\mathcal{R}_0$ and its role on global stability, in *Mathematical Approaches for Emerging and Reemerging Infectious Diseases: An Introduction*, The IMA Volumes in Mathematics and its Applications, **125** (2002), 229–250.
[8] C. Castillo-Chavez, *Mathematical and Statistical Approaches to AIDS Epidemiology*, Lecture Notes in Biomathematics, 83, 1989.
[9] C. Chiyakia, Z. Mukandavire, P. Das, F. Nyabadza, S. D. Hove Musekwa and H. Mwambi, Theoretical analysis of mixed Plasmodium malariae and Plasmodium falciparum infections with partial cross-immunity, *Journal of Theoretical Biology,* **263** (2010), 169–178.
[10] C. T. Codeço, Endemic and epidemic dynamics of cholera: The role of the aquatic reservoir, *BMC Infect Dis.*, **1** (2001), p1.
[11] C. T. Codeço and F. C. Coelho, Trends in cholera epidemiology, *PLoS Med.*, **3** (2006), e42.
[12] M. H. Cohen, A. L. French, L. Benning, A. Kovacs, K. Anastos, M. Young, H. Minko and N. A. Hessol, Causes of death among women with human immunodeficiency virus infection in the era of combination antiretroviral therapy, *Am. J. Med.*, **113** (2002), 91–98.
[13] K. Cooke and J. Yorke, Some equations modelling growth processes and gonorrhea epidemics, *Mathematical Biosciences*, **16** (1973), 75–101.
[14] N. F. Crum, R. H. Rienburgh, S. Wegner, B. K. Agan, S. A. Tasker, K. M. Spooner, A. W. Armstrong, S. Fraser and M. R. Wallace, Comparisons of causes of death and mortality rates among HIV-infected persons: Analysis of the pre-, early, and late HAART eras, *J Acquir. Immune Dec. Syndr.*, **41** (2006), 194–200.
[15] C. Elton and M. Nicholson, The ten-year cycle in numbers of the lynx in Canada, *J. Animal Ecology*, **11** (1942), 215–244.
[16] D. M. Hartley, J. G. Morris and D. L. Smith, Hyperinfectivity: A critical element in the ability of V. Cholerae to cause epidemics?, *PLoS Med.*, **3** (2005), e7.
[17] P. Hartman and C. Olech, On global asymptomatic stability of solutions of differential equations, *Trans. Amer. Math. Soc.*, **104** (1962), 154–178.
[18] H. W. Hethcote and J. A. Yorke, *Gonorrhea Transmission Dynamics and Control*, Lecture Notes in Biomathematics, 56. Springer-Verlag, Berlin, 1984.
[19] F. C. Hoppensteadt, *Mathematical Theories Among Populations: Demographics, Genetics, and Epidemics*, SIAM, 1975.

[20] J. M. Hyman, J. Li and E. A. Stanley, The differential infectivity and staged progression models for the transmission of HIV, *Mathematical Biosciences*, **155** (1999), 77–109.
[21] J. M. Hyman, J. Li and E. A. Stanley, Modeling the impact of random screening and contact tracing in reducing the spread of HIV, *Math. Biosci.*, **181** (2003), 17–54.
[22] J. M. Hyman, J. Li and E. A. Stanley, The initialization and sensitivity of multigroup models for the transmission of HIV, *Journal of Theoretical Biology*, **208** (2001), 227–249.
[23] J. M. Hyman and E. A. Stanley, Using mathematical models to understand the AIDS epidemic, *Mathematical Biosciences*, **90** (1988), 415–473.
[24] W. O. Kermack and A. G. McKendrick, A contribution to the mathematical theory of epidemics, *Proc. Roy. Soc. London B Biol. Sci.*, **115** (1927), 700–721.
[25] W. O. Kermack and A. G. McKendrick, Contributions to the mathematical theory of epidemics, part II, *Proc. Roy. Soc. London B Biol. Sci.*, **138** (1932), 55–83.
[26] W. O. Kermack and A. G. McKendrick, Contributions to the mathematical theory of epidemics, part III, *Proc. Roy. Soc. London B Biol. Sci.*, **141** (1933), 94–112.
[27] A. Lajmanovich and J. C. Yorke, A deterministic model for gonorrhea in a nonhomogeneous population, *Mathematical Biosciences*, **28** (1976), 221–236.
[28] M. Y. Li and L. Wang, Global stability in some SEIR epidemic models, in *IMA Volumes in Mathematics and its Applications* (eds. C. Castillo-Chávez et al.), **126** (2002), 295–311.
[29] A. J. Lotka, Contribution to the theory of periodic reaction, *J. Phys. Chem.*, **14** (1910), 271–274.
[30] A. J. Lotka, Analytical note on certain rhythmic relations in organic systems, *Proc. Natl. Acad. Sci. U.S.*, **6** (1920), 410–415.
[31] A. J. Lotka, *Elements of Physical Biology*, Williams and Wilkins, 1925.
[32] S. Maggi and S. Rinaldi, A second-order impact model for forest fire regimes, *Theoretical Population Biology*, **70** (2006), 174–182.
[33] N. Malunguzaa, S. Mushayabasaa, C. Chiyaka and Z. Mukandavire, Modelling the effects of condom use and antiretroviral therapy in controlling HIV/AIDS among heterosexuals, homosexuals and bisexuals, *Computational and Mathematical Methods in Medicine*, **11** (2010), 201–222.
[34] M. May, M. Gompels, V. Delpech, K. Porter, F. Poct, M. Johnson, D. Dinn, A. Palfreeman, R. Gilson, B. Gazzard, T. Hill, J. Walsh, M. Fisher, C. Orkin, J. Ainsworth, L. Bansi, A. Phillips, C. Leen, M. Nelson, J. Anderson and C. Sabin, Impact of late diagnosis and treatment on life expectancy in people with HIV-1: UK Collaborative HIV Cohort (UK CHIC) Study, *BMJ*, **343** (2011), d6016.
[35] R. M. May, Simple mathematical models with very complicated dynamics, *Nature*, **261** (1976), 459–467.
[36] W. H. McNeill, *Plagues and Peoples*, Doubleday, 1976.
[37] A. Mocroft, R. Brettle, O. Kirk, A. Blaxhult, J. M. Parkin, F. Antunes, P. Francioli, A. d'Arminio Monforte, Z. Fox, J. D. Lundgren and EuroSIDA study group, Changes in the cause of death among HIV positive subjects across Europe: results from the EuroSIDA study, *AIDS*, **16** (2002), 1663–1671.
[38] A. Mocroft, B. Ledergerber, C. Katlama, O. Kirk, P. Reiss, A. d'Arminio Monforte, B. Knysz, M. Dietrich, A. N. Phillips, J. D. Lundgren and EuroSIDA study group, Decline in the AIDS and death rates in the EuroSIDA study: An observational study, *Lancet*, **362** (2003), 22–29.
[39] Z. Mukandavire, C. Chiyaka, G. Magombedzea, G. Musukab and N. J. Malunguzaa, Assessing the effects of homosexuals and bisexuals on the intrinsic dynamics of HIV/AIDS in heterosexual settings, *Mathematical and Computer Modelling*, **49** (2009), 1869–1882.
[40] Z. Mukandavire and W. Garira, Age and sex structured model for assessing the demographic impact of mother-to-child transmission of HIV/AIDS, *Bulletin of Mathematical Biology*, **69** (2007), 2061–2092.
[41] J. D. Murray, *Mathematical Biology I: An Introduction*, 3^rd edition, Springer, 2002.
[42] F. Nakagawa, R. K. Lodwick, C. J. Smith, R. Smith, V. Cambiano, J. D. Lundgren, V. Delpech and A. N. Phillips, Projected life expectancy of people with HIV according to timing of diagnosis, *AIDS*, **26** (2012), 335–343.
[43] F. Nakagawa, M. May and A. Phillips, Life expectancy living with HIV: Recent estimates and future implications, *Curr. Opin. Infect. Dis.*, **26** (2013), 17–25.
[44] M. Nuño, Z. Feng, M. Martcheva and C. Castillo-Chavez, Dynamics of two-strain influenza with isolation and partial cross-immunity, *SIAM Journal of Applied Mathematics*, **65** (2005), 964–982.

[45] E. Odum, Fundamentals of Ecology, *Bulletin of the Torrey Botanical Club,* **82** (1955), 400–401.
[46] C. Olech, On the global stability of an autonomous system on the plane, in *On Global Univalence Theorems*, Lecture Notes in Mathematics, **977** (1983), 59–467.
[47] F. J. Palella, K. M. Delaney, A. C. Moorman, M. O. Loveless, J. Fuhrer, G. A. Satten, D. J. Aschman, S. D. Holmberg, and the HIV Outpatient Study Investigators, Declining morbidity and mortality among patients with advanced human immunodeficiency virus infection, *N. Engl. J. Med.*, **338** (1998), 853–860.
[48] C. N. Podder, O. Sharomi, A. B. Gumel, B. Song and E. Strawbridge, Mathematical analysis of a model for assessing the impact of antiretroviral therapy, voluntary testing and condom use in curtailing the spread of HIV, *Differential Equations and Dynamical Systems: International Journal for Theory, Real World Modelling and Simulations*, **19** (2011), 283–302.
[49] T. C. Porco and S. M. Blower, HIV vaccines: The effect of the mode of action on the coexistence of HIV subtypes, *Mathematical Population Studies*, **8** (2000), 205–229.
[50] M. Porta, *A Dictionary of Epidemiology*, 5^{th} edition, Oxford University Press, 2008.
[51] W. E. Ricker, Stock and Recruitment, *J. Fisher. Res. Board Can.*, **5** (1954), 559–623.
[52] R. Ross, *The Prevention of Malaria*, 2^{nd} edition, E.P Dutton and Co., 1910.
[53] D. Salmon Ceron, C. Lewden, P. Morlat, S. Bévilacqua, E. Jougla, F. Bonnet, L. Héripret, D Costagliola, T. May and G. Chêne, Liver disease as a major cause of death among HIV infected patients: Role of hepatitis C and B viruses and alcohol, *J. Hepatol.*, **42** (2005), 799–805.
[54] M. B. Schaefer, Some aspects of the dynamics of populations important to the management of commercial marine species, *Bulletin of the Inter-American Tropical Tuna Commission*, **1** (1954), 27–56.
[55] The Antiretroviral Therapy Cohort Collaboration, Life expectancy of individuals on combination antiretroviral therapy in high-income countries: A collaborative analysis of 14 cohort studies, *Lancet*, **372** (2008), 293–299.
[56] H. Thieme, *Mathematics in Population Biology*, Princeton Series in Theoretical and Computational Biology, 2003.
[57] A. Van Sighem, L. Gras, P. Reiss, K. Brinkman and F. de Wolf, Life expectancy of recently diagnosed asymptomatic HIV-infected patients approaches that of uninfected individuals, *AIDS*, **24** (2010), 1527–1535.
[58] J. X. Velasco-Hernandez and Y. H. Hsieh, Modelling the effect of treatment and behavior change in HIV-transmission dynamics, *Journal of Mathematical Biology*, **32** (1994), 233–249.
[59] V. Volterra, Variazioni e fluttuazioni del numero d'individui in specie animali conviventi, *Mem. R. Acad. Naz. dei Lincei*, **4** (1926), 31–113.
[60] V. Volterra, Variations and fluctuations of the number of individuals in animal species living together, *J. Cons. int. Explor. Mer.*, **3** (1928), 3–51.
[61] L. Wang and G.-Z. Dai, Global stability of virus spreading in complex heterogeneous networks, *SIAM J. Appl. Math*, **68** (2008), 1495–1502.

Received January 16, 2014; Accepted November 04, 2014.

E-mail address: ekthomas@umbc.edu
E-mail address: kgurski@howard.edu
E-mail address: khoffman@umbc.edu